Immunity
Article

Oral Tolerance Can Be Established via Gap Junction Transfer of Fed Antigens from CX3CR1$^+$ Macrophages to CD103$^+$ Dendritic Cells

Elisa Mazzini,[1] Lucia Massimiliano,[1] Giuseppe Penna,[1] and Maria Rescigno[1,*]
[1]Department of Experimental Oncology, European Institute of Oncology, I-20139 Milan, Italy
*Correspondence: maria.rescigno@ieo.eu
http://dx.doi.org/10.1016/j.immuni.2013.12.012

SUMMARY

Antigen-presenting cells (APCs) in the gut are apt at oral tolerance establishment at steady state and immunity after infection; complex tasks in an environment exposed to the inflammatory burden of the microbiota. Here we show an unanticipated division of labor among APCs for the establishment of oral tolerance. Chemokine receptor CX3CR1$^+$ macrophages were found to take up soluble fed antigens and quickly transfer them to CD103$^+$ dendritic cells (DCs). Antigen transfer occurred via a mechanism that was Connexin 43-dependent and required membrane transfer, indicating a physiological role of gap junctions in antigen presentation. Deletion of Connexin 43 in APCs affected antigen transfer and resulted in the inability of CD103$^+$ DCs to acquire and present antigens in vivo, to drive T regulatory cell differentiation and to induce tolerance to food antigens. This functional cooperation between intestinal phagocytes might be a mechanism to avoid the exposure of tolerogenic DCs to the intestinal microbiota.

INTRODUCTION

Oral tolerance is a process that allows an individual to be repeatedly exposed to the same food antigen (Ag) without evoking an immune response, even when the Ag is delivered systemically in combination with a strong adjuvant (Mowat, 2003). This process occurs in mesenteric lymph nodes (MLN) and requires the migration of chemokine receptor CCR7$^+$ antigen-presenting cells (APCs) from the intestine (Worbs et al., 2006). Besides classical CD11c$^-$ macrophages, at least four populations of APCs—expressing CD11c—are found in the small and large intestine having different origin and function (Coombes and Powrie, 2008; Farache et al., 2013b; Pabst and Bernhardt, 2010). A monocytic precursor gives rise to either resident CD11c$^+$ macrophages or inflammatory dendritic cells (DCs) depending on the condition found in the colon at the time of recruitment (Rivollier et al., 2012; Zigmond et al., 2012). These cells express the chemokine receptor CX3CR1 at high or intermediate amounts, respectively. CD11c$^+$CX3CR1^{hi}F4/80$^+$ monocyte-derived macrophages are anti-inflammatory in nature (Rivollier et al., 2012). They express a high quantity of interleukin-10 (IL-10), which is required for restimulation of T regulatory cells in situ (Hadis et al., 2011) and inhibit T cell proliferation via a contact-dependent mechanism (Kayama et al., 2012). CD11c$^+$CX3CR1^{hi} cells are sessile under steady-state conditions (Schulz et al., 2009) but can migrate out of the intestine if the microbiota is affected by antibiotic treatment (Diehl et al., 2013). By contrast, inflammatory DCs (CD11c$^+$CX3CR1^{int}) develop during colonic intestinal inflammation, produce large quantities of interleukin-12 (IL-12), IL-23, inducible nitric oxide synthase (iNOS), and tumor necrosis factor (TNF) and are capable of migrating to the draining lymph node and activating T helper 1 (Th1) T cells (Rivollier et al., 2012).

A second population of bona fide migratory DCs is most abundant at steady state and is characterized by the expression of CD103. CD11c$^+$CD103$^+$ DCs can be further divided into CD11b$^+$ and CD11b$^-$ cells (Bogunovic et al., 2009). CD11b$^-$CD103$^+$ cells are most likely derived from contaminant-isolated lymphoid follicles (Bogunovic et al., 2009). Conversely, CD11b$^+$CD103$^+$ cells are present in the lamina propria (LP) of the small and large intestine and migrate to the draining lymph nodes for the induction of T regulatory (Treg) cells via the release of retinoic acid (RA) and transforming growth factor-β (TGF-β) (Coombes et al., 2007; Sun et al., 2007) and the activity of Indoleamine 2,3-dioxygenase, an enzyme involved in tryptophan catabolism (Matteoli et al., 2010). Furthermore, CD11b$^+$CD103$^+$ DCs are required for the maintainance of mucosal Th17 T cells (Persson et al., 2013; Schlitzer et al., 2013).

CD103$^+$ DCs derive from a blood pre-DC precursor (Bogunovic et al., 2009; Varol et al., 2007) that expresses the α4β7 integrin and homes preferentially to the gut (Zeng et al., 2012). The tolerogenic function of CD103$^+$ DCs, as well as the expression of the αE integrin (CD103), are imparted by factors released by intestinal epithelial cells (Iliev et al., 2009a; Iliev et al., 2009b). For the above reasons, and because they are capable of migrating out of the LP to the MLN (Bogunovic et al., 2009; Schulz et al., 2009) CD103$^+$ DCs are most likely the major player in tolerance induction.

APCs are also directly involved in Ag capture from the luminal content, via the extension of dendrites between epithelial cells (Rescigno et al., 2001) particularly in the upper part of the small intestine (SI) (Chieppa et al., 2006). CX3CR1$^+$ cells are most efficient in sending protrusions out into the lumen and capture bacteria (Niess et al., 2005) and fungi (Vallon-Eberhard et al., 2006). By contrast, CD103$^+$ DCs are less frequent at extending protrusions at steady state, capture primarily bacteria and are

inefficient in taking up soluble proteins, presumably because they lack mannose receptors (Farache et al., 2013a). Thus, it is not clear how do the CD103$^+$ DCs acquire the Ag for oral tolerance induction.

In this manuscript, we analyzed which cell types are involved in the uptake of soluble Ags. We found that both intestinal epithelial cells and CX3CR1$^+$ macrophages, but not CD103$^+$ DCs, are very efficient at Ag capture from the lumen. However, only CX3CR1$^+$ macrophages transfer the Ag to CD103$^+$ DCs via a Connexin-43 (gap junction) mediated mechanism. When this transfer is inhibited by genetic deletion of Cx43 in CD11c$^+$ APCs, T regulatory cell differentiation and oral tolerance fail to be established.

RESULTS

CX3CR1$^+$ Cells Are Responsible for Antigen Uptake in the Small Intestine

The establishment of tolerance to food antigens relies on the ability of APCs to migrate through the lymphatics to the draining lymph nodes (Worbs et al., 2006). As CD103$^+$ DCs are capable of migrating out of the gut and driving the development of Treg cells (Coombes et al., 2007; Sun et al., 2007), it is likely that these cells take up the Ag from the periphery and migrate to the MLN for the establishment of oral tolerance. However, CD103$^+$ DCs, although being endowed with the capacity to contact directly the intestinal lumen, have been shown to be very inefficient in taking up soluble Ags (Farache et al., 2013a). Hence, we evaluated which subset of lamina propria phagocytes was responsible for the uptake of luminal Ags. We took advantage of *Cx3cr1*$^{GFP/+}$ genetically-targeted mice (Jung et al., 2000), which allow the efficient in vivo tracking of CX3CR1-expressing cells. *Cx3cr1*$^{GFP/+}$ mice were subjected to intestinal ligation and a fluorescent-labeled protein, Ovalbumin (OVA) conjugated with Alexa Fluor (AF) 647, was injected into the intestinal loop. After 2 hr, the loop was resected and tissues fixed and processed for imaging analysis.

As depicted in Figure 1A, the Ag colocalized preferentially with the CX3CR1$^+$ cells positioned in the apical part of the villi. The three-dimensional reconstruction of the villi clearly revealed that spots were preferentially located in the cytosol of CX3CR1$^+$ cells, but not in other CD11c$^+$ cells present in the LP (Figure 1B).

This initial observation was confirmed in a time-course experiment, where OVA-AF647 was orally administered. Small intestines were collected at different time points after feeding and processed for flow cytometry analysis; after gating on CD11c$^+$I-A-I-E^{hi} cells, CX3CR1 and CD103 markers were used to discriminate between the two main subsets of APCs in the SI, namely CD11c$^+$CX3CR1^{hi} macrophages and CD103$^+$ DCs (Figure 1C). A higher percentage of OVA$^+$ cells was observed in the CX3CR1^{hi} and CX3CR1^{int} subsets, whereas CD103$^+$ cells were almost negative. The kinetic of antigen uptake was rapid, with a peak at 3 hr after Ag administration (Figure 1D).

Furthermore, Ag uptake was unevenly distributed along the different tracts of the small bowel. Indeed, in the duodenum, Ag was equally taken up by CX3CR1^{hi} and CD45$^-$ epithelial cells, whereas in the jejunum and ileum CD45$^-$ epithelial cells outnumbered CX3CR1^{int} and CX3CR1^{hi} cells in Ag uptake, reaching almost 95%–99% of OVA-AF647$^+$ cells (Figure 1E).

Hence, we show that CX3CR1$^+$ lamina propria cells are involved in Ag uptake and accumulation in discrete intracellular compartments in the small intestine visible by immunofluorescence. Epithelial cells are the major player in Ag uptake in the jejunum and ileum, but the antigen is not localized or quickly degraded, and it is detectable only by cytofluorimetry. CD103$^+$ DCs do not seem to be involved in Ag uptake because they are negative both by immunofluorescence and by flow cytometry.

Lack of CX3CR1 Affects Antigen Uptake and Oral Tolerance Induction

APCs can extend protrusions into the intestinal lumen for bacterial uptake (Chieppa et al., 2006; Farache et al., 2013a; Niess et al., 2005; Rescigno et al., 2001). In macrophages, the extension of the luminal projections is dependent on the expression of CX3CR1. Indeed, *Cx3cr1*$^{GFP/GFP}$ mice, which have both copies of the *Cx3cr1* gene substituted by the gene coding for GFP, cannot extend the protrusions (Niess et al., 2005). Hence, we analyzed whether the presence of CX3CR1 was required for the uptake of soluble Ags, thus indicating direct uptake by these cells. *Cx3cr1*$^{GFP/+}$ and *Cx3cr1*$^{GFP/GFP}$ mice were fed with ovalbumin-AF647; after 1 hr, their intestines were removed and processed for flow cytometry staining.

The poor ability of Ag uptake by CD11b$^-$CD103$^+$ and CD11b$^+$CD103$^+$ DCs was confirmed and no difference was observed between CX3CR1-sufficient and -deficient mice (Figure 2A–B). In contrast, both CX3CR1^{int} and CX3CR1^{hi} cells showed a marked and statistically significant decrease in the uptake of OVA in *Cx3cr1*$^{GFP/GFP}$ compared to *Cx3cr1*$^{GFP/+}$ mice (Figure 2B), suggesting the involvement of CX3CR1 receptor and luminal projections in the sampling and uptake of soluble Ags from the gut lumen.

We then analyzed which cells could present the Ag after uptake. Intestinal lamina propria APC subsets were sorted from OVA-fed *Cx3cr1*^{WT} and *Cx3cr1*$^{GFP/GFP}$ mice and cocultured with CFSE-labeled naive (CD25$^-$CD4$^+$) OT-II T cells. OT-II T cells recognize the OVA$_{323–339}$ peptide in association with major histocompatibility complex (MHC) class II molecules. The sorting strategy differed as we could not use *Cx3cr1*^{GFP} to distinguish among the different subsets in wild-type (WT) animals, but we sorted the cells based on the expression of I-A-I-E, CD11c, CD11b, CD103, and F4/80 (see Figure S1A available online). T cell priming was measured as dilution of the CFSE dye due to T cell proliferation. As shown in Figure 2C, consistent with data in the literature (Rivollier et al., 2012), CD11b$^+$CD103$^+$ DCs from WT mice displayed superior ability to prime naive T cells compared to CD11b$^-$CD103$^+$, CD11c$^+$F4/80$^+$ (the equivalent of CD11c$^+$CX3CR1^{hi} macrophages) and CD11c$^-$F4/80$^+$ (classical CD11c$^-$ macrophages). In contrast, in *Cx3cr1*$^{GFP/GFP}$ mice, the priming ability of CD11b$^+$CD103$^+$ DCs was completely abolished (Figure 2D). Because we could not observe any difference in antigen presentation between CD103$^+$ DCs isolated from *Cx3cr1*^{WT} and *Cx3cr1*$^{GFP/GFP}$ mice (Figure S1B), the abolishment in antigen presentation was not due to defects in T cell priming. However, as the limit of detection of antigen presentation was 1 μg (Figure S1B), we cannot exclude that some Ag was still transferred but we could not functionally detect it. This result indirectly indicates that CD103$^+$ DCs receive the Ag from

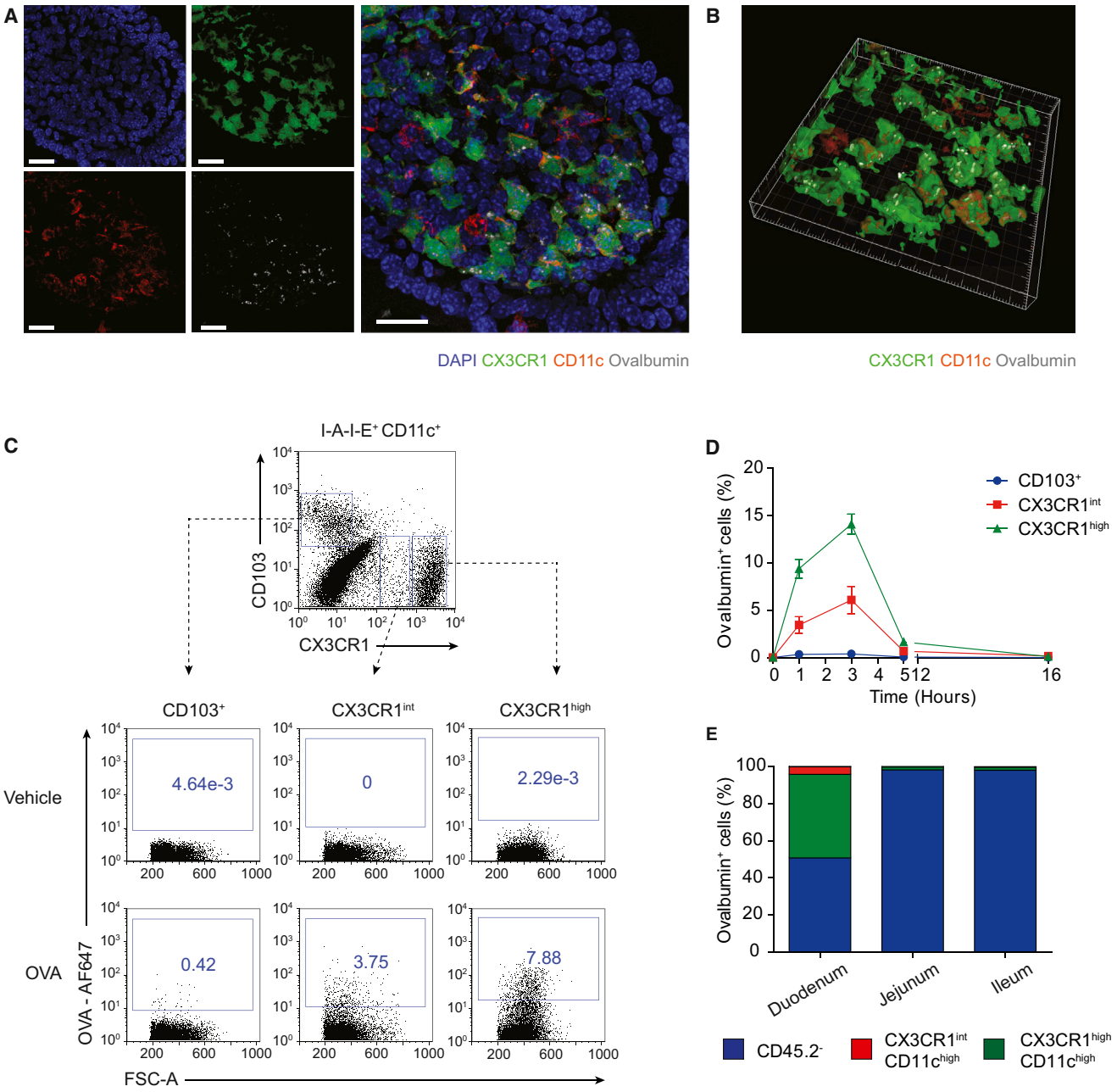

Figure 1. CX3CR1$^+$ Cells Are Responsible for Antigen Uptake in the Small Intestine

(A) A loop in the intestine of a *Cx3cr1*$^{GFP/+}$ mouse was injected with OVA-AF647. Sections represent CX3CR1 (green), OVA (gray), CD11c (red), and DAPI (blue). Scale bar represents 10 μm. Images are representative of two independent experiments, n = 2.

(B) Three-dimensional reconstruction of the SI villus with Imaris 6.1.0. The white grid marks the 3D volume, green marks CX3CR1$^+$ cells, red CD11c$^+$ cells. White dots stand for ovalbumin.

(C) OVA-AF647 or DPBS were i.g. administered to *Cx3cr1*$^{GFP/+}$ mice and intestines were collected at the indicated time points. Percentage of OVA$^+$ cells in CD103$^+$, CX3CR1^{int}, and CX3CR1^{hi} subsets is shown in (D). Results are representative of two independent experiments, each performed with three mice per group. Data are shown as mean ± SD.

(E) Duodenum, jejunum, and ileum were separately collected. Ovalbumin$^+$ cells were gated and percentages of each subset among total OVA$^+$ cells are represented; n = 4.

CX3CR1$^+$ cells because when the latter fail to take up the Ag, this affects antigen presentation by CD103$^+$ DCs.

As Ag uptake in the SI lamina propria is impaired in *Cx3cr1*$^{GFP/GFP}$ mice, we wondered whether the establishment of oral tolerance to fed Ags would be affected as well. Hence, we evaluated a delayed type hypersensitivity (DTH) response to OVA in C57BL/6, *Cx3cr1*$^{GFP/+}$, and *Cx3cr1*$^{GFP/GFP}$ mice after administration of the same Ag via the oral route. Mice were given

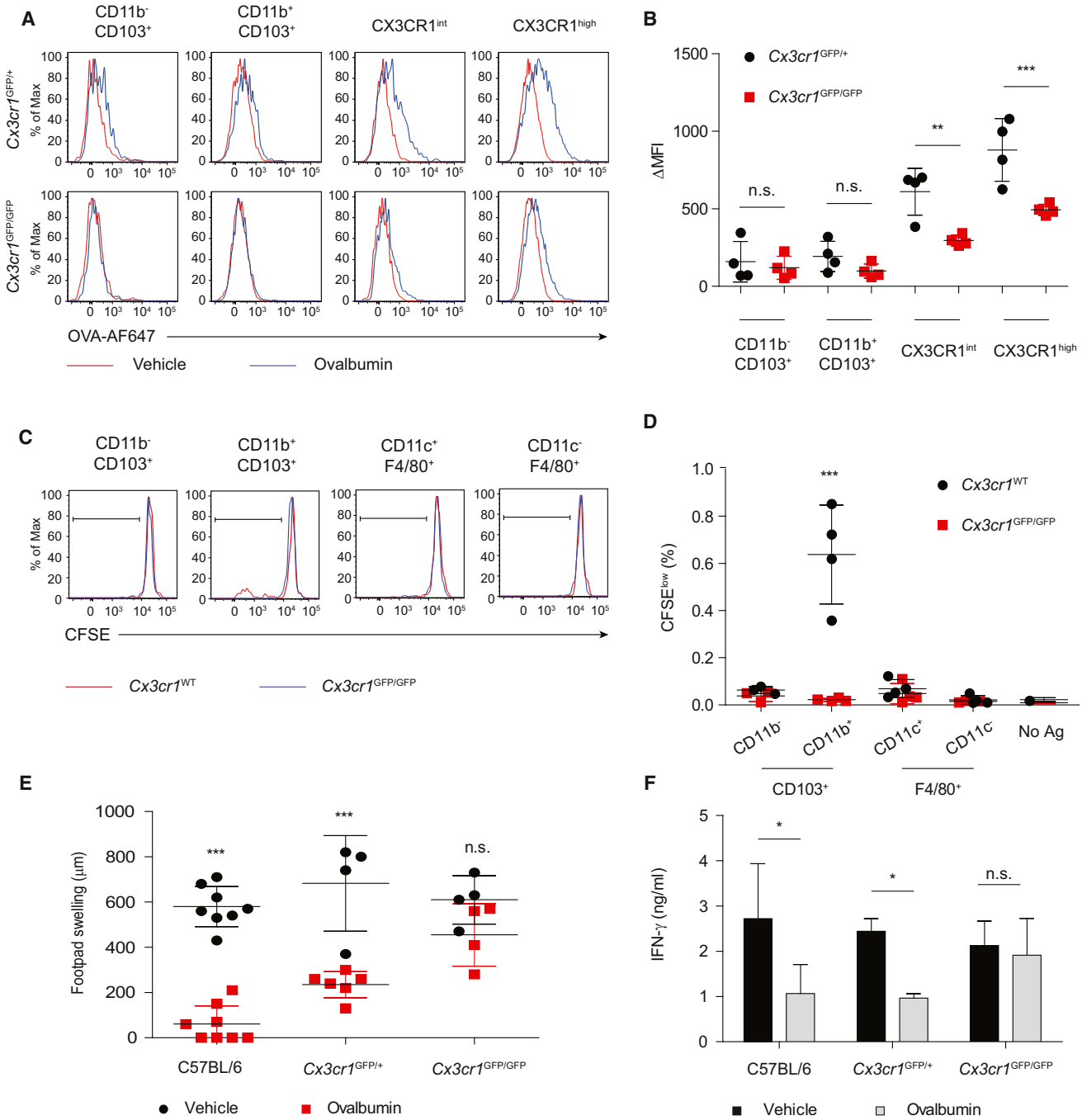

Figure 2. Lack of CX3CR1 Affects Antigen Uptake and Oral Tolerance Establishment

(A) *Cx3cr1*$^{GFP/+}$ and *Cx3cr1*$^{GFP/GFP}$ mice were i.g. administered with OVA-AF647. After 1 hr, intestines were processed for flow cytometry analysis. SI APCs were divided in four subsets, based on their expression of CD103, CX3CR1, and CD11b. Histograms show OVA-AF647 fluorescence for each subset.

(B) Data of experiment in (A) are presented as mean ± SD of the MFI (OVA-Vehicle) and are representative of two independent experiments, four mice per group.**p < 0.01; ***p < 0.001; n.s. not significant.

(C) *Cx3cr1*^{WT} and *Cx3cr1*$^{GFP/GFP}$ mice were fed with 15 mg OVA and after 4 hr APC subsets were sorted and cocultured with CFSE-labeled naive T cells for 4 days. CFSE dilution was evaluated by flow cytometry.

(D) Results in (C) are shown as mean ± SD of the percentage of DAPI^{-}CFSE^{lo} cells in the CD3^{+}CD4^{+} gate. ***p < 0.001; n.s. not significant.

(E) For C57BL/6, *Cx3cr1*$^{GFP/+}$, and *Cx3cr1*$^{GFP/GFP}$ mice, DTH response was evaluated. After 24 hr from i.f. challenge with heat-aggregated OVA, footpad swelling was measured as difference in the thickness of OVA-challenged and DPBS-injected control footpad for each mouse. Results are displayed as mean ± SD and are representative of two independent experiments, four to eight mice per group. ***p < 0.001; n.s. not significant.

(F) Splenocytes isolated from DPBS- or OVA-fed C57BL/6, *Cx3cr1*$^{GFP/+}$, and *Cx3cr1*$^{GFP/GFP}$ mice were restimulated in vitro with OVA. Supernatant was collected after 4 days and IFN-γ measured by ELISA. *p < 0.01; n.s. not significant. See also Figure S1.

OVA intragastrically (i.g.) at days −13, −10, and −7, immunized subcutaneously (s.c.) with OVA and complete Freund's adjuvant (CFA) at day 0 and challenged in the footpad (i.f.) with heat-aggregated OVA at day 7. Footpad swelling was measured after 24 hr.

Tolerance to OVA was efficiently established in C57BL/6 and at intermediate degree, in *Cx3cr1*$^{GFP/+}$ mice where oral administration of OVA resulted in a decreased DTH response. Conversely, *Cx3cr1*$^{GFP/GFP}$ mice displayed impaired induction of oral tolerance, because no significant difference was observed between vehicle- and OVA-fed mice (Figure 2E). Accordingly, splenocytes from OVA-fed C57BL/6 and *Cx3cr1*$^{GFP/+}$ mice restimulated with OVA in vitro showed a decrease in interferon-γ (IFN-γ) secretion compared to control mice, whereas no difference was observed in splenocytes derived from *Cx3cr1*$^{GFP/GFP}$ mice (Figure 2F).

Therefore, we have shown that CX3CR1-deficient mice display decreased Ag uptake by CX3CR1$^+$ cells in the small intestine and fail to develop tolerance to fed antigens in a CX3CR1 dose-dependent fashion.

CX3CR1$^+$ Macrophages and CD103$^+$ DCs Express Connexins and Communicate via Gap Junctions

We have shown above that none or little Ag was detected in CD103$^+$ DCs by flow cytometry staining; however, lamina propria CD11b$^+$CD103$^+$ cells displayed the highest capability to present Ags to naive OT-II T cells. As in the absence of CX3CR1$^+$ macrophage protrusions, CD103$^+$ DCs lost their ability to present Ags, we hypothesized that the CX3CR1$^+$ cells might be able to exchange antigenic material with CD103$^+$ cells. Because we could not detect the whole protein, we considered the possibility that the antigen might be transferred in the form of processed peptides.

Gap junctions (GJs) are channels spanning between adjacent cells that allow intercellular communication, which is their better-known function (Meşe et al., 2007). GJs play a role also in antigen presentation as they mediate the transfer of small peptides between bone-marrow-derived dendritic cells (Matsue et al., 2006) and sustain cross-presentation in acceptor cells (Neijssen et al., 2005; Saccheri et al., 2010). We found that LP CX3CR1$^+$ macrophages and CD103$^+$ DCs were in close contact in vivo and their membranes juxtapose similarly to cells communicating via GJs and display long interaction plaques (Figure S2A). Hence, we asked whether APCs in the gut might exchange material via GJs. CD11c$^+$ cells were enriched from the small intestines of C57BL/6 mice and were either loaded with calcein (a GJ diffusible dye) or labeled with the membrane-dye DDAO, which cannot diffuse through GJ. Donor (Calcein$^+$) and acceptor (DDAO$^+$) cells were cocultured, and calcein transfer to DDAO$^+$ cells was evaluated by flow cytometry. As shown in Figures 3A and 3B, calcein was transferred to DDAO$^+$CD11c$^+$ cells and the process was affected by pretreatment of cells with 1-Heptanol, a GJ-blocking agent. Maximal inhibition was obtained at a concentration of 5 mM of 1-Heptanol. This concentration was only marginally affecting DC viability (Figure S2B). We could not further inhibit the dye transfer among cells via the use of heptanol. This might suggest that other routes are also used for transferring material than just GJs, or it might highlight a limitation of the in vitro assay due to the limited survival of isolated intestinal APCs in vitro leading to phagocytosis of dead cells during the assay.

GJs are made by hemichannels (connexons) whose major constituents are connexin (Cx) proteins (Meşe et al., 2007). We first evaluated which of the 20 different murine connexins were expressed in intestinal tissues (Figure S2C and 3C). We found that six connexins were mostly expressed in the different segments of the gut (*Gjb2*, *Gjb3*, *Gjb1*, *Gja6*, *Gja1*, and *Gjc1*; Figure S2C). Hence we evaluated the relative expression of these connexins in CD11c$^+$ APCs isolated from the small intestine, MLNs, spleen, or Peyer's Patches. As shown in Figure 3C, intestinal APCs expressed a peculiar panel of the six connexins, with *Gjb1* and *Gja1* mostly expressed in all APCs.

We next sorted the different subsets of MHC-II$^+$CD11c$^+$ cells from the small intestine of *Cx3cr1*$^{GFP/+}$ mice and evaluated the expression of the six connexins.

While *Gjb2*, *Gjb3*, and *Gja6* were evenly distributed in all the subsets, other Connexins displayed a subset-specific expression. For instance, *Gjb1* and *Gjc1* were almost exclusively expressed by CX3CR1^{int} and CX3CR1^{hi} subpopulations; differently, Gja1 (the gene coding for Cx43) was mainly expressed by CX3CR1^{int} and CX3CR1^{hi} macrophages and CD11b$^+$CD103$^+$ DCs (Figure 3D), the subsets we thought might interact with each other in vivo. Indeed, when we analyzed the expression of Cx43 in the different subsets by immunofluorescence in vivo, we found that CX3CR1$^+$ macrophages and CD103$^+$ DCs had several points of interaction marked by Cx43 (Figures 3E and 3F).

Therefore, we have shown that intestinal APCs can interact with each other via GJs and that the expression of connexins is tissue- and subset-specific. Moreover, Cx43 is mostly expressed by the subsets we supposed to interact in vivo and is localized at cell-to-cell interaction sites.

Gja1$^{-/-}$ APCs Differentiate Correctly and Are Proficient in Antigen Presentation

We have shown that *Gja1* is concomitantly expressed by CX3CR1$^+$ (both CX3CR1^{int} and CX3CR1^{hi}) and CD11b$^+$CD103$^+$ DCs. To test the role of GJs, and in particular of connexin 43, in antigen transfer among APCs in the gut, we bred *Gja1*$^{fl/fl}$ mice to transgenic *Itgax-cre* mice to obtain mice (hereafter indicated as *Gja1*$^{fl/fl}$ *Itgax-cre*) in which *Gja1* was genetically deleted only in CD11c$^+$ cells (including both CX3CR1$^+$ and CD103$^+$ APCs), due to the deletion of exon 2 in the *Gja1* gene. As shown in Figures S3A and S3B, crossing of *Gja1*$^{fl/fl}$ mice with *Itgax-cre* mice led to efficient deletion of the *Gja1* gene. Efficient recombination of the *Gja1* locus was achieved in all the different intestinal subsets (Figure S3C). Lack of connexin 43 has been associated with evident defects of the hematopoietic stem cell compartment during embryonic development (Montecino-Rodriguez et al., 2000). In our model *Gja1* deletion occurred later during DC development, particularly when CD11c begins to be expressed, i.e., at the stage of pre-DCs. Nonetheless, we asked whether deletion of the *Gja1* gene in DCs might result in alterations of peripheral DC subsets.

We first analyzed small intestines of *Gja1*^{WT} and *Gja1*$^{fl/fl}$ *Itgax-cre* mice. Cells were harvested from the organs and stained to evaluate the expression of CD45.2, CD11c, MHC-II, CD103, and CD11b markers and to distinguish the three main subsets of MHC-II$^+$CD11c$^+$ cells.

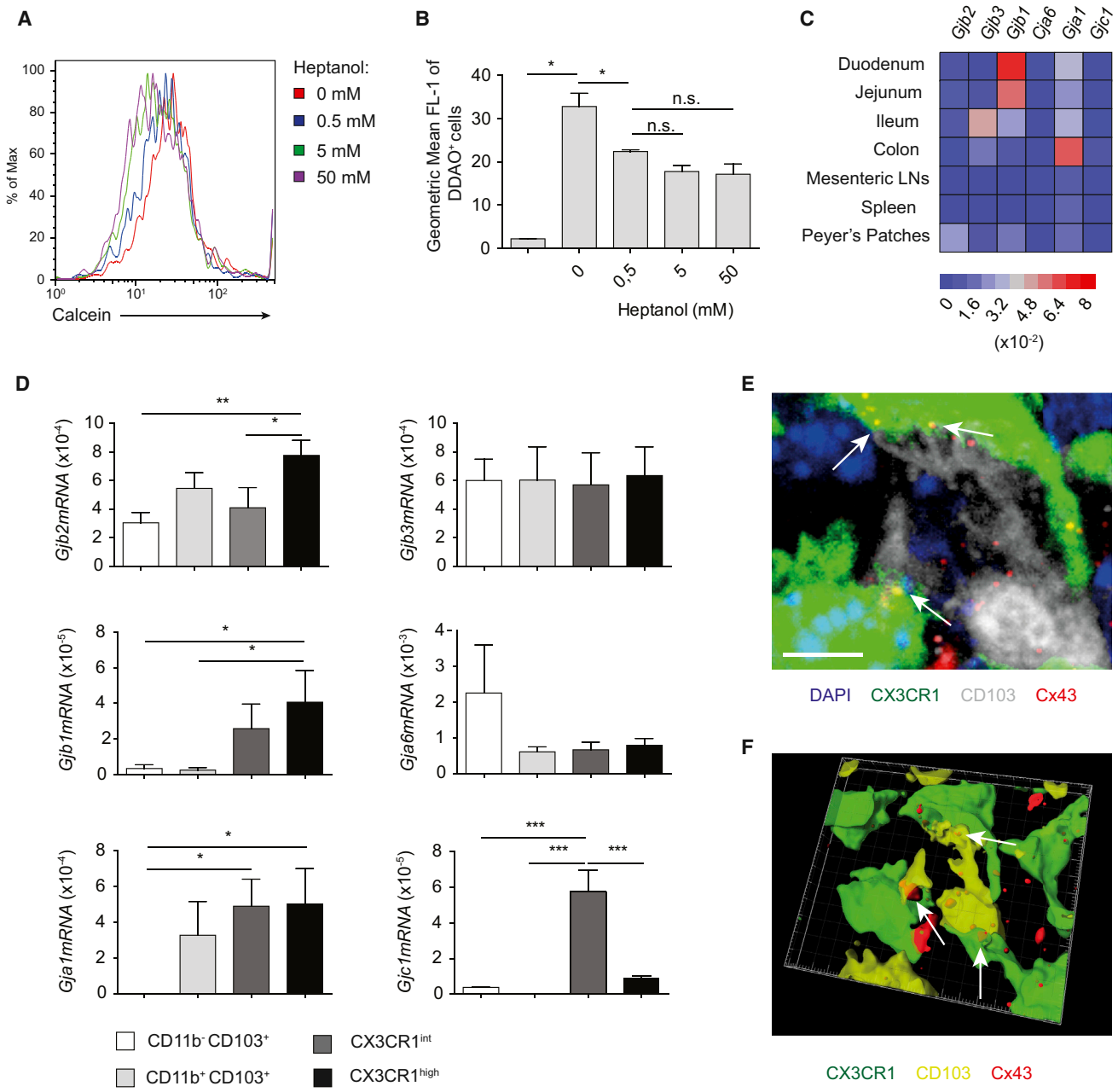

Figure 3. CX3CR1$^+$ Macrophages and CD103$^+$ DCs Express Connexins and Communicate via Gap Junctions

(A) DDAO$^+$ cells were cocultured with not labeled control cells or calcein-loaded cells. Transfer of the dye to DDAO$^+$ cells was subsequently evaluated by flow cytomtery. When indicated, increasing concentrations of 1-Heptanol were added.

(B) Mean ± SD of the geometric mean of FL-1 (Calcein) fluorescence for DDAO$^+$CD11c$^+$ cells is indicated. Pooled results from three independent experiments are shown, each of them performed with CD11c$^+$ cells obtained from four C57BL/6 mice.

(C) Connexin genes were filtered based on their relative expression to the housekeeping gene and represented as color-coded plot following the scale (from blue to red). Results represent the mean of expression values obtained for three different mice.

(D) Expression of the panel of six connexins was evaluated in sorted subsets of DCs and macrophages from the small intestine of *Cx3cr1*$^{GFP/+}$ mice (CD11b$^-$CD103$^+$, CD11b$^+$CD103$^+$, CX3CR1^{int}, and CX3CR1^{hi}). Expression results are relative to the the housekeeping *Rlp32* gene and are represented as mean ± SD of three samples derived from independent sortings. *$p < 0.05$; **$p < 0.01$; ***$p < 0.001$.

(E) Immunofluorescence staining of a small intestine tissue section for CD103, CX3CR1, and Cx43. The image represents DAPI (blue), CX3CR1 (green), Cx43 (red), and CD103 (gray). Scale bar represents 5 μm.

(F) Three-dimensional reconstruction with Imaris 6.1.0. of the small intestinal tissue stained with anti-CD103 and anti-Cx43. The white grid marks the 3D volume, green marks CX3CR1$^+$ cells, yellow CD103, red Cx43. See also Figure S2 and Table S1.

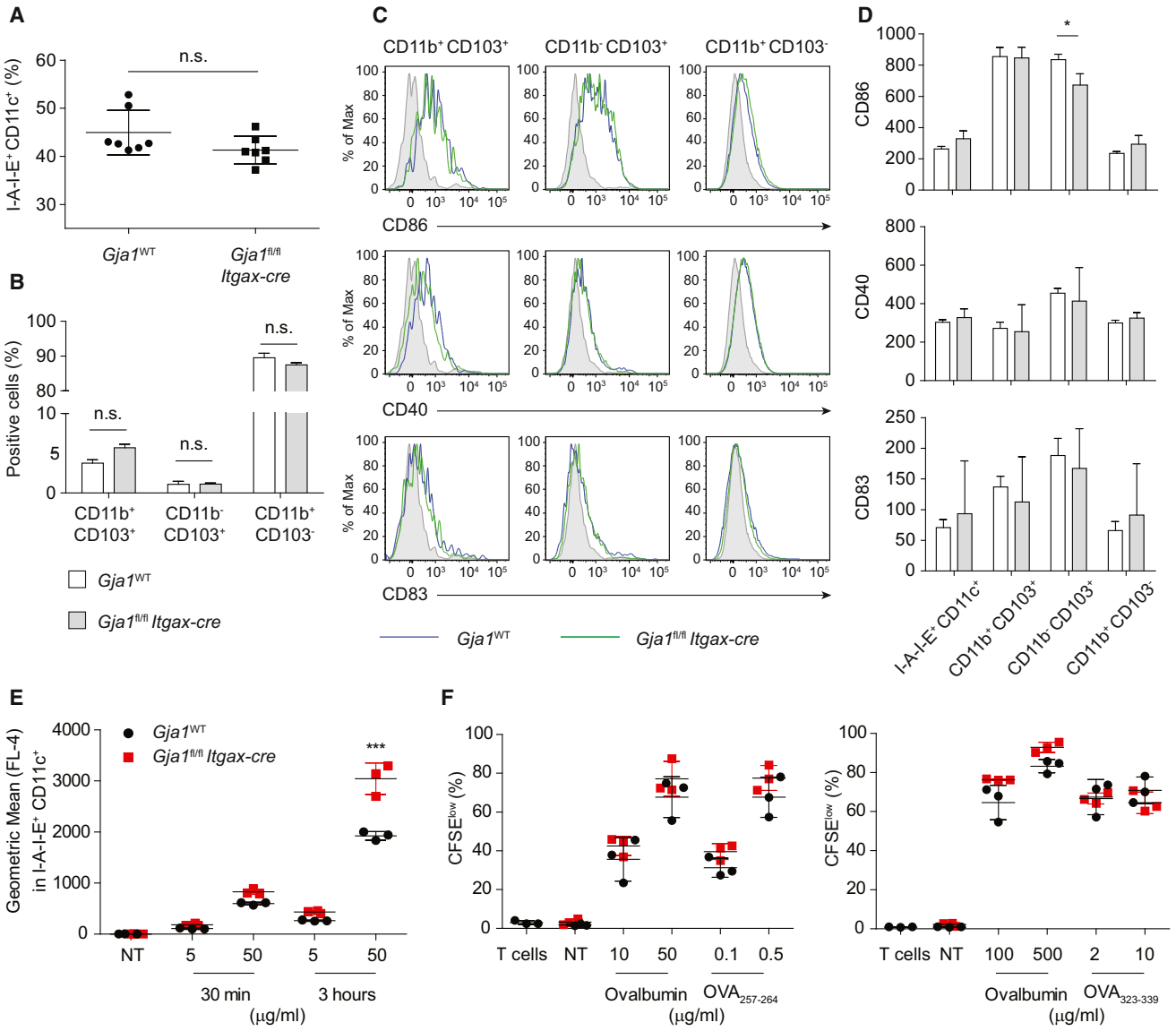

Figure 4. *Gja1*$^{-/-}$ APCs Differentiate Correctly and Are Proficient in Antigen Presentation

(A) Cells were obtained from the small intestine of *Gja1*^{WT} and *Gja1*$^{fl/fl}$ *Itgax-cre* mice. The graph represents the mean ± SD of the percentage of MHC-II$^+$CD11c$^+$ in the gate DAPI$^-$CD45.2$^+$.

(B) MHC-II$^+$CD11c$^+$ are characterized based on their expression of CD103 and CD11b. Mean percentage of each subset relative to MHC-II$^+$CD11c$^+$ gate is shown for *Gja1*^{WT} and *Gja1*$^{fl/fl}$ *Itgax-cre* mice. Results are shown as mean ± SD and are representative of two independent experiments, seven mice per group. n.s. not significant.

(C) Small intestines from *Gja1*^{WT} and *Gja1*$^{fl/fl}$ *Itgax-cre* mice were processed and expression of CD86, CD40, and CD83 costimulatory markers was evaluated. Histograms of CD86, CD40, and CD83 expression for each subset are shown. The gray line represents the isotype control, the blue line stands for *Gja1*^{WT}, the green for *Gja1*$^{fl/fl}$ *Itgax-cre*.

(D) Expression of CD86, CD40, and CD83 is reported as difference in the geometric mean between stained sample and isotype control for each subset. Data are representative of two independent experiments, three to four mice per group. *$p < 0.05$.

(E) BM-DCs were incubated with OVA-AF647 for the indicated time points. Uptake of OVA was evaluated by flow cytometry and expressed as geometric mean (FL-4) in the MHC-II$^+$CD11c$^+$ gate. Results are shown as mean ± SD and are representative of two independent experiments; ***$p < 0.001$.

(F) BM-DCs were loaded with OVA or OVA peptides and cocultured with CFSE-labeled naive OT-I or OT-II T cells. Proliferation of T cells is shown as dilution of the CFSE dye. Results represent the mean ± SD of the percentage of CFSE^{lo} cells in the gate of DAPI$^-$CD4$^+$ or DAPI$^-$CD8a$^+$. See also Figure S3.

As shown in Figures 4A and 4B, no significant differences were observed both in the percentage of MHC-II$^+$CD11c$^+$ cells and in the relative abundance of the single subsets. In addition, we evaluated the expression of costimulatory molecules, such as CD86, CD40, and CD83 in small intestinal subsets, as inhibition of Cx43 by a mimetic Cx peptide in bone-marrow-derived dendritic cells (BM-DCs) has been associated with a down-regulation of costimulatory molecules, even in the presence of

lipopolysaccharide (LPS) or IFN-γ (Matsue et al., 2006). As shown in Figures 4C and 4D, we did not observe significant differences in the expression of costimulatory molecules, except for a slight reduction in CD86 expression in $CD11b^+CD103^-$ cells.

Furthermore, we evaluated whether lack of Cx43 was impinging on the ability of dendritic cells to endocytose antigens and prime naive T cells. BM-DCs were generated ex vivo and loaded with OVA-AF647. At different time points, cells were harvested and uptake of the fluorescent Ag was evaluated by flow cytometry.

As shown in Figure 4E, *Gja1*$^{-/-}$ DCs did not display major defects in antigen uptake. Moreover, when BM-DCs were loaded with OVA or OVA peptides and cocultured with naive OT-I or OT-II T cells, no difference in $CD4^+$ or $CD8^+$ T cell priming was observed between *Gja1*$^{+/+}$ and *Gja1*$^{-/-}$ BM-DCs (Figure 4F).

Hence, *Gja1* deletion does not affect the DC balance in peripheral organs, the expression of costimulatory molecules by LP APCs, and the uptake of Ag and priming ability by ex vivo generated BM-DCs.

Connexin 43 Expression by APCs Is Required for Effective Antigen Transfer

We recently showed that, when appropriately stimulated to express Cx43, tumor cells can transfer preprocessed antigenic peptides to DCs via GJs and this is the major mechanism of cross-presentation in vivo (Saccheri et al., 2010). Analogously, as we found division of labor between $CX3CR1^+$ macrophages that take up luminal Ags and $CD103^+$ DCs that efficiently present them to T cells, we hypothesized that they might exchange antigenic material via GJs. To define whether Cx43 was involved in this process, we fed *Gja1*^{WT} and *Gja1*$^{fl/fl}$ *Itgax-cre* mice with OVA and sorted APC subsets from the small intestine after 4 hr. Subsequently, they were cocultured with CFSE-labeled naive OT-II T cells, and the capacity to present in vivo captured Ags was assessed as induction of T cell proliferation.

$CD11b^+CD103^+$ DCs isolated from *Gja1*^{WT} mice confirmed their superior ability to prime T cells compared to the other subsets. Conversely, $CD11b^+CD103^+$ DCs isolated from *Gja1*$^{fl/fl}$ *Itgax-cre* mice completely lost their capacity to present the Ag to T cells compared to the WT counterpart (Figures 5A and 5B). Of note, $F4/80^+CD11c^+$ macrophages from *Gja1*$^{fl/fl}$ *Itgax-cre* displayed increased T cell priming ability, suggesting that when they are unable to transfer the Ag to neighboring $CD103^+$ DCs, they can accumulate it and efficiently present it.

The lack of antigen presentation by *Gja1*$^{-/-}$ $CD103^+$ DCs was not due to intrinsic defects of T cell priming due to deficiency of connexin 43, because when $OVA_{323–339}$ was exogenously provided, all the intestinal APC subsets were efficiently capable of priming T cells (Figure 5C). Hence, we have shown that Cx43 is required for efficient transfer of antigenic material to $CD103^+$ DCs. This indicates that in vivo GJs have a physiological role in allowing transfer of antigenic material among cells for T cell priming.

Cx43 Allows Transfer of Surface Proteins to $CD103^+$ DCs

One important issue that rises from these results is how MHC class II peptides are transferred from a donor to an acceptor cell. Indeed, while for MHC class I crosspresentation, peptides might be exchanged via GJs from the cytosol of a donor cell to that of an acceptor cell and then be loaded on MHC class I after transport via transporter for antigen presentation (TAP) into the endoplasmic reticulum (Neijssen et al., 2007), how are peptides loaded on MHC class II molecules? An intriguing possibility is based on a recent report that whole GJ plaques can be transferred (Baker et al., 2008) from one of the two contributing cells in a preferential manner (Falk et al., 2012). Hence, we evaluated whether Cx43 was indeed exchanged together with MHC molecules from a donor to an acceptor cell. We generated a HeLa cell line overexpressing GFP-labeled murine Cx43 and coincubated it with *Gja1*$^{+/+}$ or *Gja1*$^{-/-}$ APCs. We then analyzed the proportion of GFP-Cx43 associated with the acceptor cell and because we used a human cell line, we could also evaluate the transfer of HLA class I molecules to the mouse acceptor cells. HeLa cells do not express HLA class II molecules. We found that when lamina propria APCs were incubated with cells overexpressing GFP-labeled Cx43, they could acquire Cx43 as shown by cytofluorimetry (Figure 6A) and immunofluorescence (Figure 6B). In the immunofluorescence, it is clear that $DDAO^+$ DCs are decorated with Cx43-GFP at the site of interaction with GFP^+ HeLa cells. We did not permeabilize the cells and assessed that together with Cx43-GFP, the acceptor cells acquired also surface HLA-ABC molecules from the donor cells, ruling out a simply phagocytic process (Figure 6C). Consistently, GFP^- APCs, as well as APCs incubated with the parental HeLa cell line, not expressing murine Cx43, were lacking the expression of HLA. The transfer of cell membranes required cell contact, because it was not occurring when the cells were physically separated with a transwell (Figure 6D), suggesting that it is not dependent on exosome release by the donor cell. The transfer was decreased when the acceptor cells were not expressing Cx43 and was associated only to the $CD11b^+$ $CD103^+$ DC subset (Figure 6E), suggesting that there is a still-unknown mechanism associated to $CD103^+$ DCs and not to $CX3CR1^+$ macrophages that controls the transfer and defines a directionality. This is consistent with the finding that $CX3CR1^+$ macrophages lose the ability to present the lumen-derived OVA peptides as presumably they transfer them to the acceptor cell.

Cx43 Expression by Intestinal APCs Is Required for the Conversion of Ag-Specific Treg Cells and Oral Tolerance Establishment

Because $CD11b^+CD103^+$ DCs have been regarded as the only migratory subset able to polarize Treg cells in the MLN at steady state, we asked whether in the absence of Ag transfer between macrophages and DCs, Treg cell polarization was affected. Hence, Gja1^{WT} and *Gja1*$^{fl/fl}$ *Itgax-cre* mice were injected intravenously (i.v.) with CFSE-labeled $CD45.1^+$ naive OT-II T cells and subsequently fed with OVA on 2 consecutive days. After 4 days, MLNs and spleens were removed and Treg cell conversion was evaluated by flow cytometry (Figure 7A). As shown in Figures 7B and 7C, a decrease in the percentage of Treg cells was observed in the MLN of *Gja1*$^{fl/fl}$ *Itgax-cre* mice. This correlated with an increase in the frequency of OT-II T cells in *Gja1*$^{fl/fl}$ *Itgax-cre* mice (Figure 7C, second panel), suggesting that at the concentration used, the Ag could

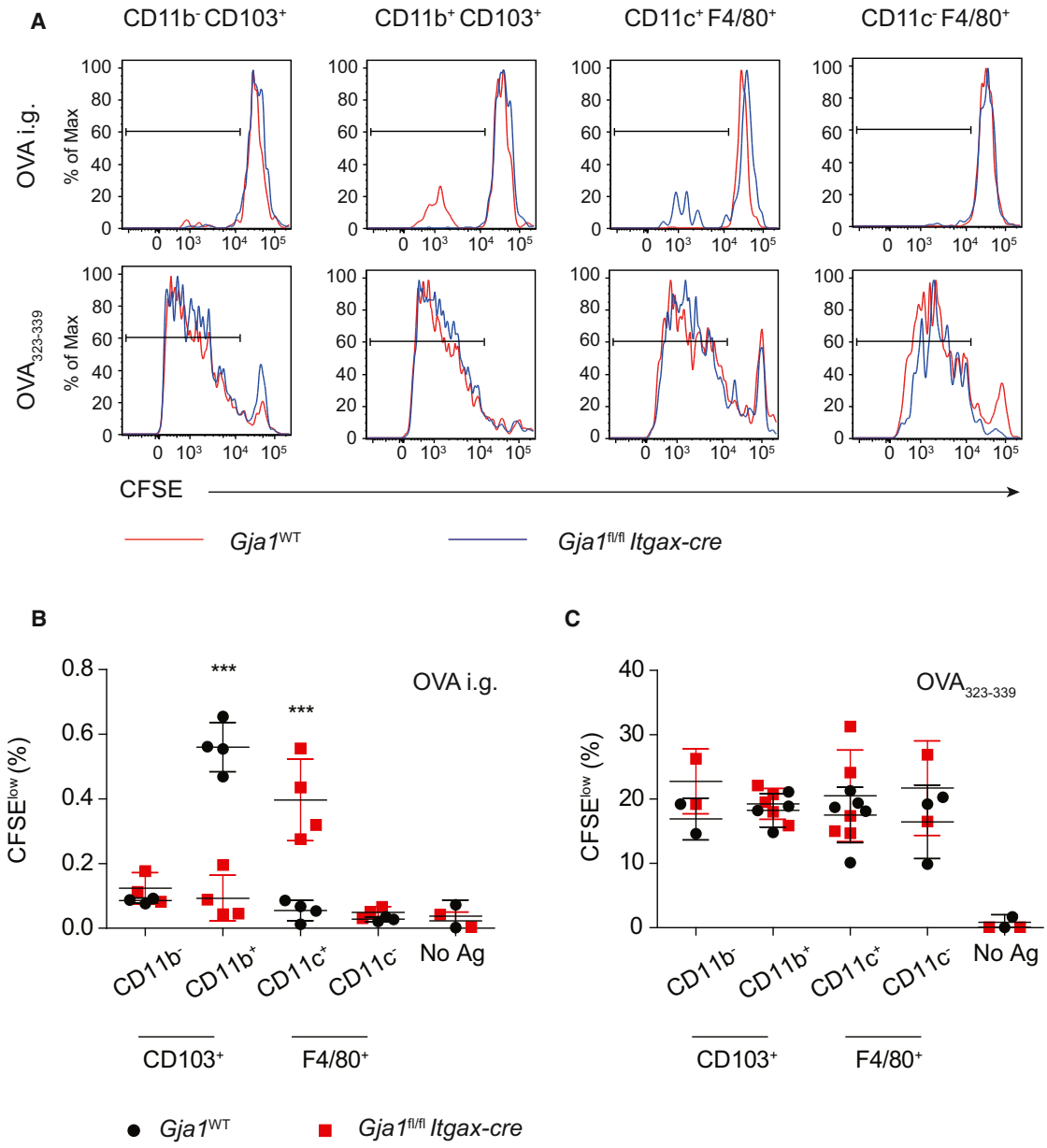

Figure 5. Connexin 43 Expression by APCs Is Required for Effective Antigen Transfer

(A) *Gja1*^{WT} and *Gja1*$^{fl/fl}$ *Itgax-cre* mice were i.g. administered with 15 mg OVA and after 4 hr APC subsets were sorted and cocultured with CFSE-labeled naive $CD25^-CD4^+$ OT-II T cells for 4 days. CFSE dilution was evaluated by flow cytometry. $OVA_{323–339}$-loaded APCs are used as positive controls.

(B) Results in (A) are shown as mean ± SD of the percentage of $DAPI^-CFSE^{lo}$ cells in the $CD3^+CD4^+$ gate. ***$p < 0.001$; n.s. not significant.

reach the draining lymph node (presumably in a free form); however, this was not sufficient to drive Treg cell induction, confirming previous data that CCR7-dependent migration of antigen-loaded DCs is required for a regulatory tolerogenic response (Worbs et al., 2006).

Given the reduction of $CD4^+$ Treg cells in the mesenteric lymph nodes, we hypothesized that also tolerance induction might be impaired in *Gja1*$^{fl/fl}$ *Itgax-cre* mice.

To evaluate a possible contribution of *Gja1* deletion in $CD11c^+$ cells in oral tolerance induction, we administered OVA i.g. to *Gja1*^{WT} and *Gja1*$^{fl/fl}$ *Itgax-cre* mice and then carried out a DTH response. Thus, mice were administered three times with 1 mg OVA every second day and immunized s.c. with OVA mixed to CFA after 7 days. Mice were then challenged i.f. with heat-aggregated OVA or DPBS as a control, and footpad swelling was measured as a readout for the DTH after 24 hr.

As expected, decrease in the footpad swelling of control *Gja1*^{WT} mice was reported after OVA feeding, compared to vehicle-fed mice. Conversely, *Gja1*$^{fl/fl}$ *Itgax-cre* mice showed impairment in oral tolerance establishment, as no significant difference was observed between ovalbumin- and vehicle-fed mice (Figure 7D).

Altogether, these results indicate that, when *Gja1* is deleted in CD11c$^+$ cells, APCs cannot exchange antigenic material, and this results in defects in Treg cell differentiation and oral tolerance establishment, a further indication of a physiological role of GJ in Ag transfer and presentation.

DISCUSSION

Here we have described that APCs in the gut are highly specialized in function, but cooperate for the establishment of oral tolerance. We have shown that soluble food Ags are taken up by CX3CR1$^+$ macrophages and by epithelial cells, but not by CD103$^+$ DCs. Interestingly, uptake of antigen by CX3CR1$^+$ cells was observed primarily in the upper part of the small intestine (duodenum), where the mucus layer is more patchy. However, CD103$^+$ cells could present the Ag. Because we could never detect the whole OVA in CD103$^+$ DCs, the Ag must have been transferred—in an undetectable and presumably processed form—to the latter. Data in the literature have shown that mice lacking CX3CR1 are not capable of extending protrusions into the gut lumen (Niess et al., 2005). Hence, we thought we had a major tool to assess whether these cells were required for taking up fed antigen and for eventually transferring it to CD103$^+$ DCs. We found that in mice lacking CX3CR1 (*Cx3cr1*$^{GFP/GFP}$ mice), CX3CR1$^+$ cells were devoid of antigen. This correlated with the failure of CD103$^+$ DCs to acquire the antigen and to mount oral tolerance toward it. This indirectly indicates that CD103$^+$ DCs do not acquire the antigen from cells other than the CX3CR1$^+$ cells. A recent publication has shown that deficiency of CX3CR1 results in defects in oral tolerance establishment because macrophages are unable to produce IL-10 and to restimulate T regulatory cells (Hadis et al., 2011). Here, we have integrated this finding by showing that deficiency of CX3CR1 also results in the reduced ability of taking up the antigen and of transferring it to CD103$^+$ DCs.

It has been recently suggested that Goblet cells can serve as a gateway for the uptake of small antigens (McDole et al., 2012). These cells have also been shown to be in close interaction with CD103$^+$ cells and to handle them the captured antigen (McDole et al., 2012). However, the interaction between Goblet cells and CD103$^+$ DCs has been shown to be a rare event (Farache et al., 2013a) and might be relevant particularly at high concentration of the antigen. Our finding of a requirement for CX3CR1 to take up the antigen and for the subsequent transfer to CD103$^+$ DCs suggests that transfer of antigen between Goblet cells and CD103$^+$ cells is dispensable for oral tolerance induction.

Because we could not detect the whole Ag in CD103$^+$ DCs, either via immunofluorescence or via cytofluorimetry, but we could observe antigen presentation after in vivo administration of OVA, we supposed that the Ag might be transferred in a processed or undetectable form. Even though DCs have been shown to connect via the formation of long-range tunneling nanotubules (Watkins and Salter, 2005), we found that the transfer of the antigenic peptides depended on the expression of Cx43 in APCs, thus suggesting a contribution of GJs rather than nanotunneling in Ag transfer. GJs are involved in a series of intercellular communication processes and have been shown to participate in several immunological functions in vitro, including the transfer of antigenic peptides (Mendoza-Naranjo et al., 2007; Neijssen et al., 2005), the activation of DCs (Matsue et al., 2006) and T cells (Mendoza-Naranjo et al., 2011), the function of Treg cells (Bopp et al., 2007), and the interaction between Treg cells and DCs (Luckey et al., 2012). We have previously shown that GJs are required for efficient induction of antitumor immunity in vivo as silencing of connexin 43—the major component of GJ—in tumor cells abolishes the development of systemic antitumor immunity (Saccheri et al., 2010). Here we found that mice lacking Cx43 only in APCs were uncapable of mounting oral tolerance in response to administration of OVA. This correlated with the inability of CD103$^+$ DCs to acquire the antigen in vivo and to present it to T cells. We also found that when CX3CR1$^+$ macrophages could not transfer the antigen to CD103$^+$ DCs, they were much better at antigen presentation, indicating that at steady state they are incapable of presenting the Ag primarily because they quickly transfer it to adjacent CD103$^+$ DCs. One question that remained unsolved was how the antigen entered the MHC class II presentation pathway. One possibility is related to the recent findings that whole GJ plaques could be transferred from one of the two contributing cells (Baker et al., 2008) in a preferential manner (Falk et al., 2012). Endocytosed vesicles can then be targeted for macroautophagy and lysosomal degradation, and this might allow loading of peptides on MHC II molecules. Alternatively, during the internalization of the plaque, MHC class II-peptide complexes might be transferred to the acceptor cell membrane. We found that when LP APCs are incubated with cells overexpressing GFP-labeled Cx43, they can receive Cx43, as well as MHC molecules, from the donor cell. This process is a characteristic associated only to the CD103$^+$ DCs, suggesting that there is a directionality in the transfer of the GJs. The finding that HLA molecules from the donor cell could be detected on the surface of the acceptor cell suggests that the whole complex can be acquired and exposed by the donor cell. This is reminiscent of a mechanism of transfer of preformed peptide-MHC complexes between neighboring cells called trogocytosis (Joly and Hudrisier, 2003) that is used to crossdress DCs for induction of immunity to viruses (Smyth et al., 2012; Wakim and Bevan, 2011). We now propose that this mechanism is dependent on Cx43 and is a physiological mechanism required to transfer antigens between gut APCs that are specialized in their function. This process might require a functional pore because it is inhibited by the GJ blocker heptanol.

In conclusion, we show an unanticipated functional cooperation between CX3CR1$^+$ macrophages and CD103$^+$ DCs in the uptake, transfer and presentation of soluble antigens that is mediated by Cx43. This indicates that in vivo Cx43 plays a major physiological role in immune responses and in antigen exchange among APCs via transfer of MHC-peptide complexes, presumably via trogocytosis. It remains to be established how the directionality of antigen transfer is achieved. We also have shown that epithelial cells' uptake of antigen is not finalized to tolerance induction, but it might be likely that epithelial cells are primarily involved in the uptake and degradation of soluble proteins for energy harvest.

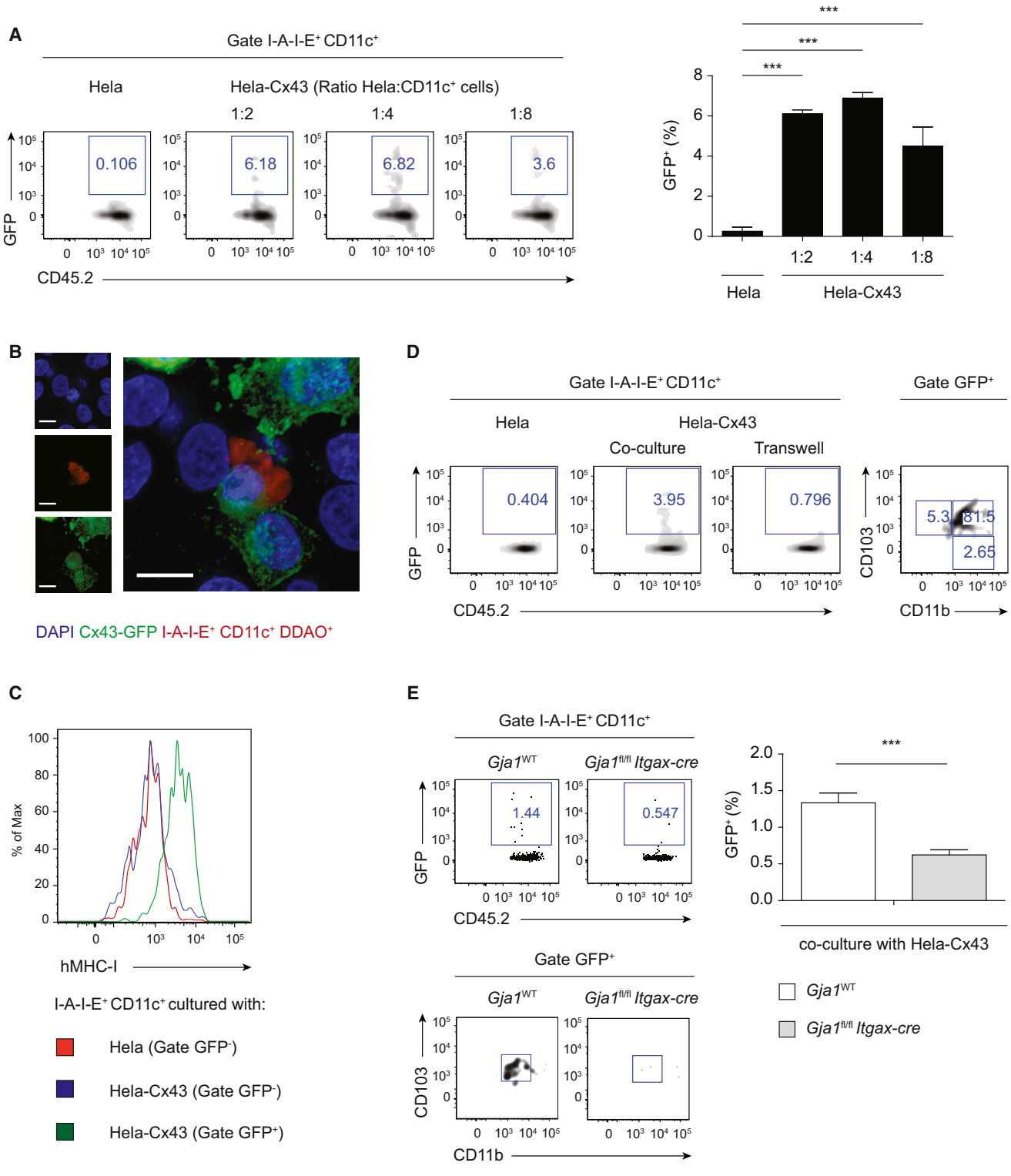

Figure 6. Cx43 Allows Transfer of Surface Proteins to CD103+ DCs

(A) HeLa-Cx43 or control HeLa cells were cocultured with CD11c+ cells enriched from the small intestine of C57BL/6 mice at different ratios (1:2, 1:4, 1:8). After 12 hr, cells were stained with anti-CD45.2, CD11c, and MHC-II. Density plots represent the percentage of GFP+ cells in the I-A-I-E+CD11c+ gate. Data are shown as mean ± SD for three independent samples.

(B) HeLa or HeLa-Cx43 were cocultured with DDAO-labeled I-A-I-E+CD11c+ cells sorted from the SI and visualized by confocal microscopy. Blue, DAPI; red DDAO; green Cx43-GFP. Scale bar represents 15 μm.

(legend continued on next page)

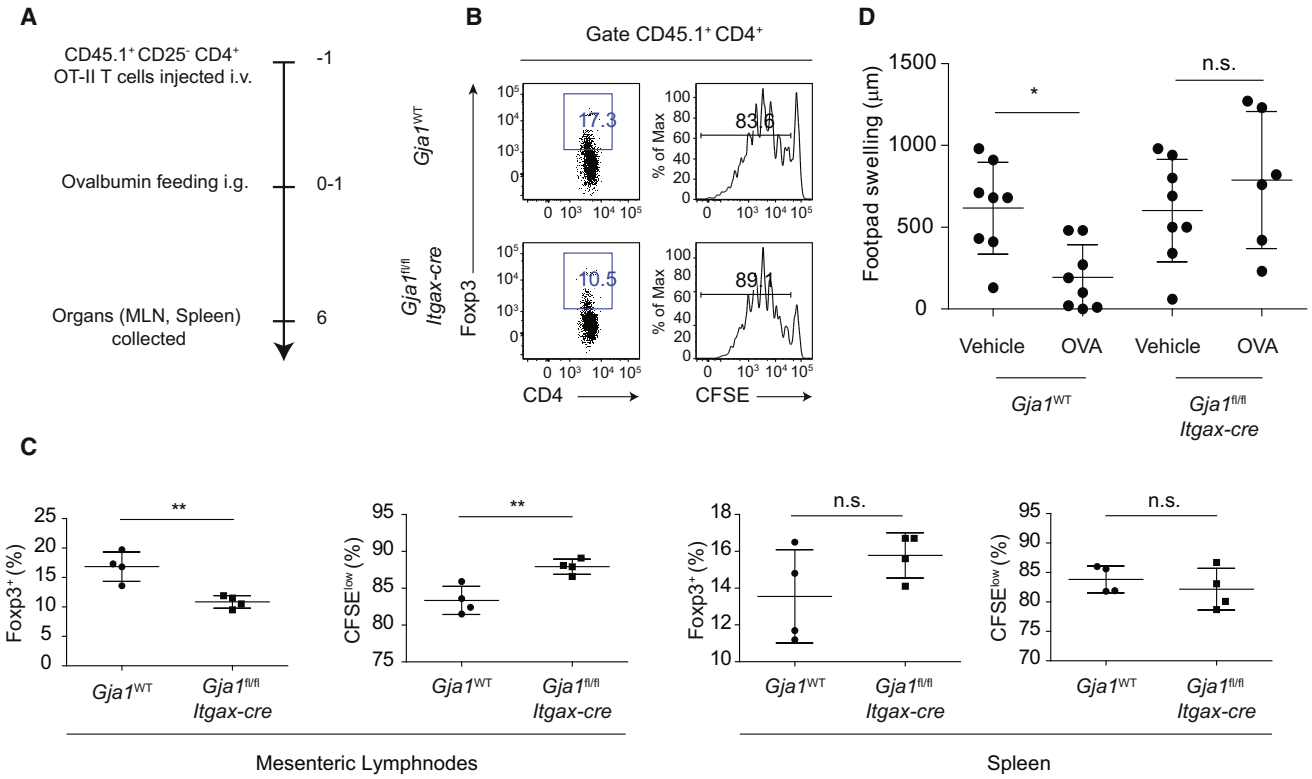

Figure 7. Cx43 Expression by Intestinal APCs Is Required for the Conversion of Ag-Specific Tregs and Oral Tolerance Establishment

(A) *Gja1*^{WT} and *Gja1*$^{fl/fl}$ *Itgax-cre* mice were i.v. injected with 2 × 10^6 CFSE$^+$ naive OT-II Ly5.1$^+$ CD25$^-$ CD4$^+$ T cells and subsequently i.g. administered with 15 mg of ovalbumin. At day 6, MLNs and spleens were collected and processed for flow cytometry staining.

(B) Foxp3 expression and T cell proliferation were analyzed in the Ly5.1$^+$ cells by flow cytometry.

(C) Results in (B) are represented as percentage ± SD of Foxp3$^+$ or CFSE^{lo} cells in the CD45.1$^+$CD4$^+$ gate. n = 4.

(D) *Gja1*^{WT} and *Gja1*$^{fl/fl}$ *Itgax-cre* were subjected to a DTH protocol. After i.f. challenge with heat-aggregated ovalbumin, footpad swelling was measured as difference in the thickness of OVA-challenged and PBS-injected control footpad for each mouse and expressed as mean ± SD n = 6–8 mice per group. *p < 0.05, n.s. not significant.

EXPERIMENTAL PROCEDURES

Intestinal Loop and OVA Feeding

Cx3cr1$^{GFP/+}$ mice were anesthetized with 2.5% Avertin for the duration of the experiment. Segments of the small intestine were exposed and ligated at both extremities with surgical thread. We injected 40 μg of OVA-AF647 (Molecular Probes) into the loop, removed the intestines after 2 hr, and processed them for immunofluorescence staining (see Supplemental Experimental Procedures). When indicated, 250 μg of OVA-AF647 were administered i.g. in 200 μl DPBS with a feeding needle. Animals were bred and maintained in our SPF (Specific Pathogen Free) animal facility. All experiments were performed in accordance with the guidelines established in the Principles of Laboratory Animal Care (directive 86/609/EEC).

Flow Cytometry and Cell Sorting

Cells were isolated from the different tissues as indicated in the Supplemental Experimental Procedures.

For flow cytometry staining or cell sorting, cells were incubated with anti-FcR antibody (clone 24G2; BD Biosciences) and stained with the following primary antibodies: anti-CD45.2 (clone 104, eBioscience), CD11c (clone HL3, BD PharMingen), MHC-II (clone M5/114.15.2, eBioscience), CD103 (clone M290, BD PharMingen), CD11b (clone M1/70, eBioscience), CD86 (clone GL1, BD PharMingen), CD40 (clone HM40-3, BD PharMingen), and CD83 (clone Michel-19, BD PharMingen). DAPI was added to exclude dead cells.

Samples were acquired with FACSCanto (BD Biosciences) and analyzed by FlowJo (Treestar).

Cells were sorted by FACSAria (BD Biosciences) into CD11b$^-$CD103$^+$, CD11b$^+$CD103$^+$, CD11b$^+$CX3CR1^{int}, and CD11b$^+$CX3CR1^{hi} populations. From *Gja1*^{WT} and *Gja1*$^{fl/fl}$ *Itgax-cre* mice, MHC-II$^+$ cells were sorted into CD11c$^+$CD11b$^-$CD103$^+$, CD11c$^+$CD11b$^+$CD103$^+$, CD11c$^+$CD11b$^+$F4/80$^+$, and CD11c$^-$CD11b$^+$F4/80$^+$ subsets. When indicated, mice were fed with 15 mg ovalbumin and intestines collected after 4 hr.

Collected cells were sorted in complete medium (RPMI, 10% FBS, 1% Penicillin-Streptomycin, 1% Glutamine, 50 μM β-Mercaptoethanol) and

(C) After coculture with HeLa or HeLa-Cx43, I-A-I-E$^+$CD11c$^+$ cells were stained for human MHC-I. Histograms show human MHC-I expression for I-A-I-E$^+$CD11c$^+$ cultured with HeLa (red) or HeLa-Cx43 (blue, GFP$^-$; green, GFP$^+$).

(D) CD11c-enriched APCs were cocultured with HeLa or HeLa-Cx43 cells, in contact or separated by a transwell. Plots represent the percentage of GFP$^+$ cells in the I-A–I-E$^+$CD11c$^+$ subset. In the right plot, expression of CD103 and CD11b markers is shown for GFP$^+$ cells.

(E) HeLa and HeLa-Cx43 were cocultured with I-A-I-E$^+$CD11c$^+$ APCs isolated from the intestine of *Gja1*^{WT} and *Gja1*$^{fl/fl}$ *Itgax-cre* mice. Cells were then stained with anti-CD45.2, CD11c, MHC-II, CD103, and CD11b. Plots represent GFP$^+$ cells in the I-A-I-E$^+$CD11c$^+$ gate and the expression of CD11b and CD103 markers by this subset. Data are represented as mean ± SD of GFP$^+$ cells in each subset. ***p < 0.001.

subsequently centrifuged at 2,000 rpm for 10'. When proceeding with RNA extraction, cells were lysed in RTL Plus Buffer (Quiagen) and processed as indicated in the Supplemental Experimental Procedures.

T Cells-DC Cocultures

BM-DCs were generated as described in the Supplemental Experimental Procedures. For DC-T cell cocultures, BM-DCs were loaded with OVA or OVA peptides (MHC-I restricted $OVA_{257–264}$ or MHC-II restricted $OVA_{323–339}$, Invivogen) for 4 hr. We seeded 5×10^3 BM-DCs in a 96-well plate and cocultured them with Ag-specific T cells at a ratio of 1:10. $CD25^-CD4^+$ and $CD25^-CD8^+$ naive T cells were obtained from the spleens of OT-I and OT-II mice, respectively. They were enriched with beads (Miltenyi Biotec) to a purity >95%–98% and labeled with 5 μM CFSE (Molecular Probes). After 3 days of coculture, cells were stained with anti-CD3 (clone 145-2C11, eBioscience), CD4 (clone H129.19, BD PharMingen), and CD8 (clone 53-6.7, BD PharMingen). DAPI was added before acquisition to exclude dead cells.

Sorted APCs were coculture with CFSE-labeled naive $CD25^-CD4^+$ OT-II T cells at a ratio of 1:5 for 4 days.

Oral Tolerance

Mice were fed i.g. with 1 or 20 mg of OVA in 200 μl DPBS on days 13, 10, and 7 before OVA-CFA immunization. Mice were immunized s.c. with 50 ug OVA in 100 μl PBS-CFA emulsion. After 7 days, mice were challenged by s.c. injection of 250 μg heat-aggregated OVA in 20 μl of PBS in the left hind footpad. Right footpad received PBS as a control. OVA-specific DTH was determined by footpad swelling 24 hr after challenge with heat-aggregated OVA. Footpad swelling was measured as difference in the thickness of OVA-challenged and DPBS-injected control footpad for each mouse.

Total splenocytes were subsequently isolated and restimulated in vitro with 1 mg/ml OVA. Red blood cells were lysed with a hypotonic red cell lysis buffer, and 5×10^4 cells per each well were seeded in a 96-well plate. Supernatants were collected after 4 days and IFN-γ measured by CBA FACSArray (BD Biosciences).

Calcein Transfer Assay

$CD11c^+$ cells were enriched from small intestines of C57BL/6 mice and were divided into two pools: one was labeled with 15 μM DDAO (Molecular Probes) for 15 min at room temperature; the second was labeled with 0.5 μM Calcein-AM (Molecular Probes) in serum-free medium for 30 min at 37°C. After labeling, cells were extensively washed in complete medium.

The two pools were cocultured for 30 min and calcein transfer was evaluated by flow cytometry. When indicated, cells were pretreated with 1-Heptanol (Sigma Aldrich) at different concentration (0.5, 5, and 50 mM) for 2 hr.

Adoptive T Cell Transfer and Antigen Oral Feeding

$CFSE^+$-labeled naive T cells $CD4^+CD25^-$ (2×10^6) isolated from OT-II $Ly5.1^+$ mice were adoptively transferred intravenously into *Gja1*^{WT} and *Gja1*$^{fl/fl}$ *Itgax-cre* $Ly5.2^+$ recipients at day 0. At days 1 and 2, mice received an i.g. administration of 15 mg of OVA (grade III; Sigma-Aldrich). On day 6, MLNs and spleens were collected from $Ly5.2^+$ hosts; proliferation and Foxp3 expression were analyzed in the $Ly5.1^+$ transplanted cells by flow cytometry.

Cells were permeabilized with the eBioscience Fix-Perm buffer for 1 hr according to manufacturer's instructions. Cells were subsequently stained in Wash-Perm Buffer (eBioscience) with anti-CD45.1 (clone A20, eBioscience), CD4 (clone H129.19, BD PharMingen), and Foxp3 (clone FJK-16 s, eBioscience). Samples were acquired with FACSCanto (BD Biosciences) and analyzed with FlowJo (Tristar).

Coculture of HeLa Cells and $CD11c^+$ Cells

HeLa cells were transfected to express murine Cx43 (see Supplemental Experimental Procedures). Twenty-four hr after transfection, transfected cells (HeLa-Cx43) and control HeLa cells were seeded in 96-well plates and cocultured with $CD11c^+$ cells enriched from the small intestine or I-A-I-E^+CD11c^+ cells sorted from the small intestine of *Gja1*^{WT} and *Gja1*$^{fl/fl}$ *Itgax-cre* mice. In some experiments, a transwell with 3.0 μm pores was used to separate HeLa and lamina propria cells.

After 12 hr, cells were collected and stained with anti-CD45.2, CD11c, MHC-II, CD103, and CD11b. Human MHC-I was stained with an anti-HLA-ABC (clone W6/32, Exbio). DAPI was added to exclude dead cells.

For immunofluorescence, HeLa-Cx43 and HeLa cells were seeded in a 8-well Permanox slide and cocultured for 24 hr with I-A-I-E^+CD11c^+ labeled with 1 μM DDAO (Molecular Probes). Slides were then fixed in PFA 4% for 15 min.

Statistics

Results were represented as mean ± SD. Statistical significance between two groups was determined by the nonpaired Student's t test while the comparison of multiple groups was carried out by two-way ANOVA followed by Bonferroni post-test using GraphPad Prism software. *$p < 0.05$, **$p < 0.01$, *** $p < 0.001$, n.s. not significant.

SUPPLEMENTAL INFORMATION

Supplemental Information includes three figures, one table, and Supplemental Experimental Procedures and can be found with this article online at http://dx.doi.org/10.1016/j.immuni.2013.12.012.

ACKNOWLEDGMENTS

M.R. is supported by grants of the European Commission (ERC Dendroworld), the Italian Foundation for Cancer Research (AIRC), the International Association for Cancer Research (AICR), and the Italian Ministry of Health (Ricerca Finalizzata).

Received: June 21, 2013
Accepted: December 31, 2013
Published: January 23, 2014

REFERENCES

Baker, S.M., Kim, N., Gumpert, A.M., Segretain, D., and Falk, M.M. (2008). Acute internalization of gap junctions in vascular endothelial cells in response to inflammatory mediator-induced G-protein coupled receptor activation. FEBS Lett. *582*, 4039–4046.

Bogunovic, M., Ginhoux, F., Helft, J., Shang, L., Hashimoto, D., Greter, M., Liu, K., Jakubzick, C., Ingersoll, M.A., Leboeuf, M., et al. (2009). Origin of the lamina propria dendritic cell network. Immunity *31*, 513–525.

Bopp, T., Becker, C., Klein, M., Klein-Hessling, S., Palmetshofer, A., Serfling, E., Heib, V., Becker, M., Kubach, J., Schmitt, S., et al. (2007). Cyclic adenosine monophosphate is a key component of regulatory T cell-mediated suppression. J. Exp. Med. *204*, 1303–1310.

Chieppa, M., Rescigno, M., Huang, A.Y., and Germain, R.N. (2006). Dynamic imaging of dendritic cell extension into the small bowel lumen in response to epithelial cell TLR engagement. J. Exp. Med. *203*, 2841–2852.

Coombes, J.L., and Powrie, F. (2008). Dendritic cells in intestinal immune regulation. Nat. Rev. Immunol. *8*, 435–446.

Coombes, J.L., Siddiqui, K.R., Arancibia-Cárcamo, C.V., Hall, J., Sun, C.M., Belkaid, Y., and Powrie, F. (2007). A functionally specialized population of mucosal CD103+ DCs induces Foxp3+ regulatory T cells via a TGF-beta and retinoic acid-dependent mechanism. J. Exp. Med. *204*, 1757–1764.

Diehl, G.E., Longman, R.S., Zhang, J.X., Breart, B., Galan, C., Cuesta, A., Schwab, S.R., and Littman, D.R. (2013). Microbiota restricts trafficking of bacteria to mesenteric lymph nodes by CX(3)CR1(hi) cells. Nature *494*, 116–120.

Falk, M.M., Fong, J.T., Kells, R.M., O'Laughlin, M.C., Kowal, T.J., and Thévenin, A.F. (2012). Degradation of endocytosed gap junctions by autophagosomal and endo-/lysosomal pathways: a perspective. J. Membr. Biol. *245*, 465–476.

Farache, J., Koren, I., Milo, I., Gurevich, I., Kim, K.W., Zigmond, E., Furtado, G.C., Lira, S.A., and Shakhar, G. (2013a). Luminal bacteria recruit CD103+ dendritic cells into the intestinal epithelium to sample bacterial antigens for presentation. Immunity *38*, 581–595.

Farache, J., Zigmond, E., Shakhar, G., and Jung, S. (2013b). Contributions of dendritic cells and macrophages to intestinal homeostasis and immune defense. Immunol. Cell Biol. *91*, 232–239.

Hadis, U., Wahl, B., Schulz, O., Hardtke-Wolenski, M., Schippers, A., Wagner, N., Müller, W., Sparwasser, T., Förster, R., and Pabst, O. (2011). Intestinal tolerance requires gut homing and expansion of FoxP3+ regulatory T cells in the lamina propria. Immunity *34*, 237–246.

Iliev, I.D., Mileti, E., Matteoli, G., Chieppa, M., and Rescigno, M. (2009a). Intestinal epithelial cells promote colitis-protective regulatory T-cell differentiation through dendritic cell conditioning. Mucosal Immunol. *2*, 340–350.

Iliev, I.D., Spadoni, I., Mileti, E., Matteoli, G., Sonzogni, A., Sampietro, G.M., Foschi, D., Caprioli, F., Viale, G., and Rescigno, M. (2009b). Human intestinal epithelial cells promote the differentiation of tolerogenic dendritic cells. Gut *58*, 1481–1489.

Joly, E., and Hudrisier, D. (2003). What is trogocytosis and what is its purpose? Nat. Immunol. *4*, 815.

Jung, S., Aliberti, J., Graemmel, P., Sunshine, M.J., Kreutzberg, G.W., Sher, A., and Littman, D.R. (2000). Analysis of fractalkine receptor CX(3)CR1 function by targeted deletion and green fluorescent protein reporter gene insertion. Mol. Cell. Biol. *20*, 4106–4114.

Kayama, H., Ueda, Y., Sawa, Y., Jeon, S.G., Ma, J.S., Okumura, R., Kubo, A., Ishii, M., Okazaki, T., Murakami, M., et al. (2012). Intestinal CX3C chemokine receptor 1(high) (CX3CR1(high)) myeloid cells prevent T-cell-dependent colitis. Proc. Natl. Acad. Sci. USA *109*, 5010–5015.

Luckey, U., Schmidt, T., Pfender, N., Romer, M., Lorenz, N., Martin, S.F., Bopp, T., Schmitt, E., Nikolaev, A., Yogev, N., et al. (2012). Crosstalk of regulatory T cells and tolerogenic dendritic cells prevents contact allergy in subjects with low zone tolerance. The Journal of allergy and clinical immunology *130*, 781–797.e711.

Matsue, H., Yao, J., Matsue, K., Nagasaka, A., Sugiyama, H., Aoki, R., Kitamura, M., and Shimada, S. (2006). Gap junction-mediated intercellular communication between dendritic cells (DCs) is required for effective activation of DCs. J. Immunol. *176*, 181–190.

Matteoli, G., Mazzini, E., Iliev, I.D., Mileti, E., Fallarino, F., Puccetti, P., Chieppa, M., and Rescigno, M. (2010). Gut CD103+ dendritic cells express indoleamine 2,3-dioxygenase which influences T regulatory/T effector cell balance and oral tolerance induction. Gut *59*, 595–604.

McDole, J.R., Wheeler, L.W., McDonald, K.G., Wang, B., Konjufca, V., Knoop, K.A., Newberry, R.D., and Miller, M.J. (2012). Goblet cells deliver luminal antigen to CD103+ dendritic cells in the small intestine. Nature *483*, 345–349.

Mendoza-Naranjo, A., Saéz, P.J., Johansson, C.C., Ramírez, M., Mandakovic, D., Pereda, C., López, M.N., Kiessling, R., Sáez, J.C., and Salazar-Onfray, F. (2007). Functional gap junctions facilitate melanoma antigen transfer and cross-presentation between human dendritic cells. J. Immunol. *178*, 6949–6957.

Mendoza-Naranjo, A., Bouma, G., Pereda, C., Ramírez, M., Webb, K.F., Tittarelli, A., López, M.N., Kalergis, A.M., Thrasher, A.J., Becker, D.L., and Salazar-Onfray, F. (2011). Functional gap junctions accumulate at the immunological synapse and contribute to T cell activation. J. Immunol. *187*, 3121–3132.

Meşe, G., Richard, G., and White, T.W. (2007). Gap junctions: basic structure and function. J. Invest. Dermatol. *127*, 2516–2524.

Montecino-Rodriguez, E., Leathers, H., and Dorshkind, K. (2000). Expression of connexin 43 (Cx43) is critical for normal hematopoiesis. Blood *96*, 917–924.

Mowat, A.M. (2003). Anatomical basis of tolerance and immunity to intestinal antigens. Nat. Rev. Immunol. *3*, 331–341.

Neijssen, J., Herberts, C., Drijfhout, J.W., Reits, E., Janssen, L., and Neefjes, J. (2005). Cross-presentation by intercellular peptide transfer through gap junctions. Nature *434*, 83–88.

Neijssen, J., Pang, B., and Neefjes, J. (2007). Gap junction-mediated intercellular communication in the immune system. Prog. Biophys. Mol. Biol. *94*, 207–218.

Niess, J.H., Brand, S., Gu, X., Landsman, L., Jung, S., McCormick, B.A., Vyas, J.M., Boes, M., Ploegh, H.L., Fox, J.G., et al. (2005). CX3CR1-mediated dendritic cell access to the intestinal lumen and bacterial clearance. Science *307*, 254–258.

Pabst, O., and Bernhardt, G. (2010). The puzzle of intestinal lamina propria dendritic cells and macrophages. Eur. J. Immunol. *40*, 2107–2111.

Persson, E.K., Uronen-Hansson, H., Semmrich, M., Rivollier, A., Hägerbrand, K., Marsal, J., Gudjonsson, S., Håkansson, U., Reizis, B., Kotarsky, K., and Agace, W.W. (2013). IRF4 transcription-factor-dependent CD103(+) CD11b(+) dendritic cells drive mucosal T helper 17 cell differentiation. Immunity *38*, 958–969.

Rescigno, M., Urbano, M., Valzasina, B., Francolini, M., Rotta, G., Bonasio, R., Granucci, F., Kraehenbuhl, J.P., and Ricciardi-Castagnoli, P. (2001). Dendritic cells express tight junction proteins and penetrate gut epithelial monolayers to sample bacteria. Nat. Immunol. *2*, 361–367.

Rivollier, A., He, J., Kole, A., Valatas, V., and Kelsall, B.L. (2012). Inflammation switches the differentiation program of Ly6Chi monocytes from antiinflammatory macrophages to inflammatory dendritic cells in the colon. J. Exp. Med. *209*, 139–155.

Saccheri, F., Pozzi, C., Avogadri, F., Barozzi, S., Faretta, M., Fusi, P., and Rescigno, M. (2010). Bacteria-induced gap junctions in tumors favor antigen cross-presentation and antitumor immunity. Sci. Transl. Med. *2*, 44ra57.

Schlitzer, A., McGovern, N., Teo, P., Zelante, T., Atarashi, K., Low, D., Ho, A.W., See, P., Shin, A., Wasan, P.S., et al. (2013). IRF4 transcription factor-dependent CD11b+ dendritic cells in human and mouse control mucosal IL-17 cytokine responses. Immunity *38*, 970–983.

Schulz, O., Jaensson, E., Persson, E.K., Liu, X., Worbs, T., Agace, W.W., and Pabst, O. (2009). Intestinal CD103+, but not CX3CR1+, antigen sampling cells migrate in lymph and serve classical dendritic cell functions. J. Exp. Med. *206*, 3101–3114.

Smyth, L.A., Hervouet, C., Hayday, T., Becker, P.D., Ellis, R., Lechler, R.I., Lombardi, G., and Klavinskis, L.S. (2012). Acquisition of MHC:peptide complexes by dendritic cells contributes to the generation of antiviral CD8+ T cell immunity in vivo. J. Immunol. *189*, 2274–2282.

Sun, C.M., Hall, J.A., Blank, R.B., Bouladoux, N., Oukka, M., Mora, J.R., and Belkaid, Y. (2007). Small intestine lamina propria dendritic cells promote de novo generation of Foxp3 T reg cells via retinoic acid. J. Exp. Med. *204*, 1775–1785.

Vallon-Eberhard, A., Landsman, L., Yogev, N., Verrier, B., and Jung, S. (2006). Transepithelial pathogen uptake into the small intestinal lamina propria. J. Immunol. *176*, 2465–2469.

Varol, C., Landsman, L., Fogg, D.K., Greenshtein, L., Gildor, B., Margalit, R., Kalchenko, V., Geissmann, F., and Jung, S. (2007). Monocytes give rise to mucosal, but not splenic, conventional dendritic cells. J. Exp. Med. *204*, 171–180.

Wakim, L.M., and Bevan, M.J. (2011). Cross-dressed dendritic cells drive memory CD8+ T-cell activation after viral infection. Nature *471*, 629–632.

Watkins, S.C., and Salter, R.D. (2005). Functional connectivity between immune cells mediated by tunneling nanotubules. Immunity *23*, 309–318.

Worbs, T., Bode, U., Yan, S., Hoffmann, M.W., Hintzen, G., Bernhardt, G., Förster, R., and Pabst, O. (2006). Oral tolerance originates in the intestinal immune system and relies on antigen carriage by dendritic cells. J. Exp. Med. *203*, 519–527.

Zeng, R., Oderup, C., Yuan, R., Lee, M., Habtezion, A., Hadeiba, H., and Butcher, E.C. (2012). Retinoic acid regulates the development of a gut-homing precursor for intestinal dendritic cells. Mucosal Immunol. *6*, 847–856.

Zigmond, E., Varol, C., Farache, J., Elmaliah, E., Satpathy, A.T., Friedlander, G., Mack, M., Shpigel, N., Boneca, I.G., Murphy, K.M., et al. (2012). Ly6C hi monocytes in the inflamed colon give rise to proinflammatory effector cells and migratory antigen-presenting cells. Immunity *37*, 1076–1090.